

# MIRCO-STRUCTURES OF RF SURFACES IN THE ELECTRON-BEAM-WELD REGIONS OF NIOBIUM\*

R.L. Geng<sup>†‡</sup>, J. Knobloch, H. Padamsee  
Laboratory of Nuclear Studies, Cornell University, Ithaca, NY 14853

## Abstract

Micro-structures of RF surfaces in the electron-beam-weld (EBW) regions of niobium samples were studied. These surfaces were polished with different techniques, namely buffered chemical polish (1:1:2 BCP) and electrolytic polish (EP). It was found that there are three distinctively different regions near the EBW, characterized by different grain sizes, shapes, and orientations. Strikingly, we found grain boundaries within the EBW are nicely lined up so that they form an angle of about 60 degree with respect to the weld seam. Upon being polished with BCP, these grain boundaries evolve into micro-steps with sharp edges, due to preferential etching of different crystallographic planes. There is evidence that the step height increases up to possibly more than 30 microns with repeated chemical polish. In contrast to the result with BCP, dimensions of surface irregularities were reduced with EP and sharp edges were rounded off. These observations have important implications in explanations of the high-field-Q-drop of niobium superconducting cavities.

## 1 INTRODUCTION

The performance of a superconducting cavity used in modern accelerators is intimately connected with the condition of its RF surface. For this reason, different surface preparation techniques have been developed to get an ideal surface. A newly fabricated bulk niobium cavity is usually etched either by chemical polish (1:1:2 BCP) or by electrolytic polish (EP) [1].

In case of cavities made of bulk niobium, different cavity parts are welded together with electron-beam-welding technique. Because of large amount of heat deposition, the electron-beam-weld (EBW) region is expected to distinguish itself from a virgin niobium region. The significance to differentiate EBW regions from virgin niobium regions is underlined by the fact that these regions are subjected to either peak electric fields (iris regions) or peak magnetic fields (equator regions) for modern niobium cavities with elliptical shapes.

In this paper, micro-structures of RF surfaces near the EBW regions of different niobium samples are studied. This work is motivated by the experimental studies of a newly observed fundamental cavity performance limita-

tion, the so called high-field-Q-drop [2]. Recent experiments show that the same cavity would have quite different performance with different surface treatments [3]. It is therefore of interest to have detailed studies on RF surfaces following various preparations.

## 2 SAMPLES AND PREPARATIONS

Two EBW samples were studied, one of which, denoted as S3C1-3-EQUATOR, is cut from the equator of a well etched S-band cavity and the other is a flat sample, denoted as TWC-155E, for weld testing with typical parameters. The raw material of these two samples came from the same batch (by Teledyne Wah Chang) with a starting RRR of 300 and a starting thickness of about 1.6 mm.

The two EBW samples were welded with the so called "Rhombic raster weld" technique [4] with a beam voltage of 50kV. The beam current and beam traveling speed (or cavity rotational speed) are 22 mA and 30 cm/min for the S3C1-3-EQUATOR sample, and 30 mA and 45 cm/min for the TWC-155E sample respectively. The apparent width of weld seams, as viewed with naked eyes, is about 4-5 mm. Prior to the study described in this paper, the S3C1-3-EQUATOR sample has been well etched ( $> 100 \mu\text{m}$ ) with 1:1:2 BCP at 15 °C; while the TWC-155E sample was not etched at all.

In this study, samples were etched by 1:1:2 BCP (see [1] for detailed information about the mixture), and/or EP (with a mixture of HF(49% wt.) and H<sub>2</sub>SO<sub>4</sub>(96% wt.) in a volume ratio of 10:105). The temperature of the acid was in the range of 11 - 16 °C for BCP and 25 - 34 °C for EP respectively. For BCP, the acid was agitated manually at an interval of about 5 minutes; while for EP, the electrolyte was agitated continuously yet gently with a spin bar driven by a magnetic stirrer. In case of EP, the anode-cathode voltage was regulated to be constantly at 12 V. With this configuration, the anode current was almost constant with a slow increase as a result of temperature rise with time, due to heat generated by the flowing current. The anode current density ranged from 25 - 30 mA/cm<sup>2</sup>. The average surface removal rate is 1  $\mu\text{m}/\text{min}$  for BCP and 0.3  $\mu\text{m}/\text{min}$  for EP respectively.

## 3 THREE REGIONS NEAR AN EBW

After enough surface removal by etching, three regions can be easily distinguished near an EBW, namely the *weld region*, the *heat-affected region* and the *non-affected region*.

\* Work supported by the National Science Foundation.

<sup>†</sup> on leave from IHIP, Peking University, Beijing 100871, PRC.

<sup>‡</sup> Email: rg58@cornell.edu

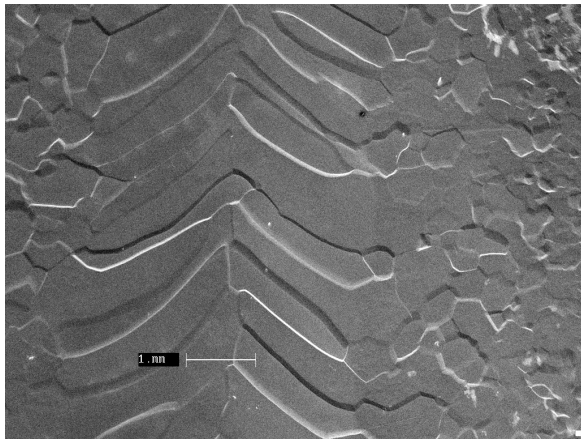


Figure 1: The SEM photo of the weld and heat-affected region of the sample TWC-155E after a surface removal of  $177\mu\text{m}$  by BCP. The length of the scale bar in the figure is 1mm.

Grains in different regions have different sizes, shapes and orientations. Fig. 1 shows the weld surface of the sample TWC-155E after a surface removal of  $117\mu\text{m}$  by BCP. The middle part of the photo shows the weld region and the region next to the weld shows the heat-affected region. In the weld region, Grain boundaries are lined up in a way that they form an angle of about  $60^\circ$  with respect to the weld joint line. Grains have elongated dimensions, comparable to the half width of the weld, in the lining-up direction. In the heat-affected region, grains have smaller dimensions compared to that in the weld region and take random orientations. The overall width of the weld and heat-affected region is 12 mm.

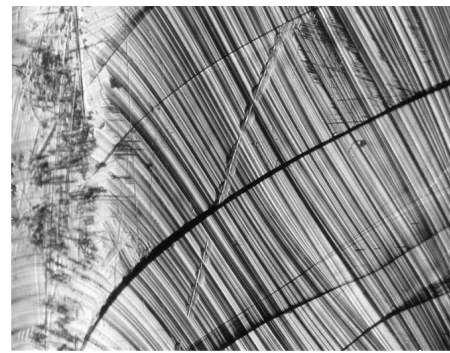
A non-affected region is one that is not affected by the heat deposition during electron-beam welding. Therefore it bears the same appearance as that of a virgin niobium (see Fig. 6(a)). Grains in this region are even smaller than that in the heat-affected region and their orientations are highly random.

## 4 EVOLUTION OF WELD SURFACES WITH REPEATED ETCHING

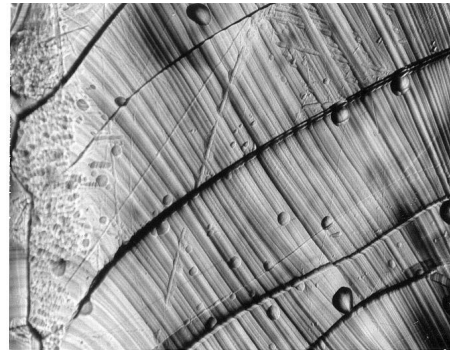
### 4.1 Weld surfaces after repeated BCP

The sample TWC-155E was etched by BCP repeatedly in a step by step manner. Fig. 2<sup>1</sup> illustrates the evolution of its weld surface with an increased amount of surface removal. Fig. 2(a) shows the virgin surface, featuring mechanical scratches and weld ripples. Grain boundaries are also clearly visible. The left border of the photo approximately coincides with the joint line of the weld. Note the grain boundary crossing over Fig. 2(a) from the lower left corner to the upper right corner has already shown a step nature at this stage. After a  $30\mu\text{m}$  surface removal by BCP,

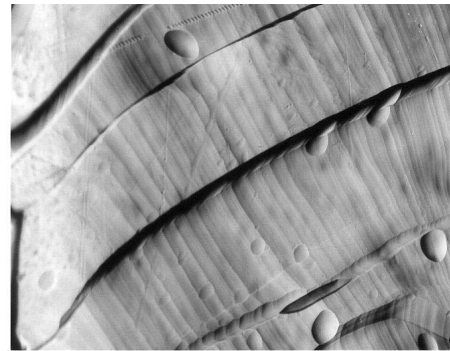
<sup>1</sup>All the photos in this section were taken with an optical microscope. Each photo covers an area of  $1770\mu\text{m}$  wide by  $1370\mu\text{m}$  high.



(a)



(b)



(c)



(d)

Figure 2: The weld surface of the sample TWC-155E with different surface removal by BCP. Virgin surface (a). After a surface removal of  $30\mu\text{m}$  (b);  $117\mu\text{m}$  (c);  $250\mu\text{m}$  (d). The left border of the photos coincides with the weld joint line.

scratches are not effectively removed. In addition, many circular defects with various dimensions emerge, as shown

in Fig. 2(b). After a surface removal of  $117\mu\text{m}$ , surface scratches are totally abated, as shown in Fig. 2(c). However, circular defects, especially those starting with larger dimensions, still sit on the surface. This suggests that these circular defects are actually spherical ones embedded in the surface layer of the weld region. Only after a surface removal of  $250\mu\text{m}$  are circular defects gone (see Fig. 2(d)).

Although it is scratch free and circular (or spherical), to be accurate) defect free after a surface removal of  $250\mu\text{m}$ , the RF surface of the weld region is far less than perfect at this stage. As can be seen from Fig. 2(d), the step crossing over from the lower left corner to the upper right corner of the photo has grown into a much bigger one, with a very sharp edge, due to preferential etching of different crystallographic planes. One should also note that the emerging bean-shaped defect,  $310\mu\text{m}$  long by  $50\mu\text{m}$  wide, sitting near the lower right corner in Fig. 2(c) has evolved into a much bigger defect,  $850\mu\text{m}$  long by  $250\mu\text{m}$  wide in Fig. 2(d) as a result of an extra  $133\mu\text{m}$  etching.

#### 4.2 Weld surfaces after BCP followed by repeated EP

After having received a surface removal of  $117\mu\text{m}$ , half of the sample TWC-155E was etched by EP in a step by step manner.

Fig. 3 shows the evolution of its weld surface with an increased amount of surface removal by EP. Note the tie-shaped feature dominating the center of the photo is a plateau with respect to the area surrounding it. Again, the left border of the photo approximately coincides with the joint line of the weld.

It turns out that EP is very effective in removing spherical defects. As can be seen by comparing Fig. 3(a) and Fig. 3(b), an etching of  $26\mu\text{m}$  by EP suffices to remove those spherical defects.

Another important effect of EP lies in the fact that those sharp edges left behind by BCP are rounded off to a large extent, as can be seen from the evolution of the step edge of the plateau. There is also evidence that the height of the plateau is reduced by EP. The height of the plateau was roughly measured by adjusting the distance between the object and the lens to get the best focus when looking at different areas. Qualitatively speaking, more surface removal by EP, more pronounced rounding-off effect on step edges and more step height reduction.

#### 4.3 Weld surfaces after EP followed by repeated BCP

In this study, the sample S3C1-3-EQUATOR was first etched by EP until a surface removal of  $100\mu\text{m}$  was reached. The sample was then etched by BCP in a step by step manner. Fig. 4 illustrates the evolution of its weld surface with an increased amount of surface removal by BCP. The linear feature starting from the center of the photo to right is a going-down step if walking from the upper to the

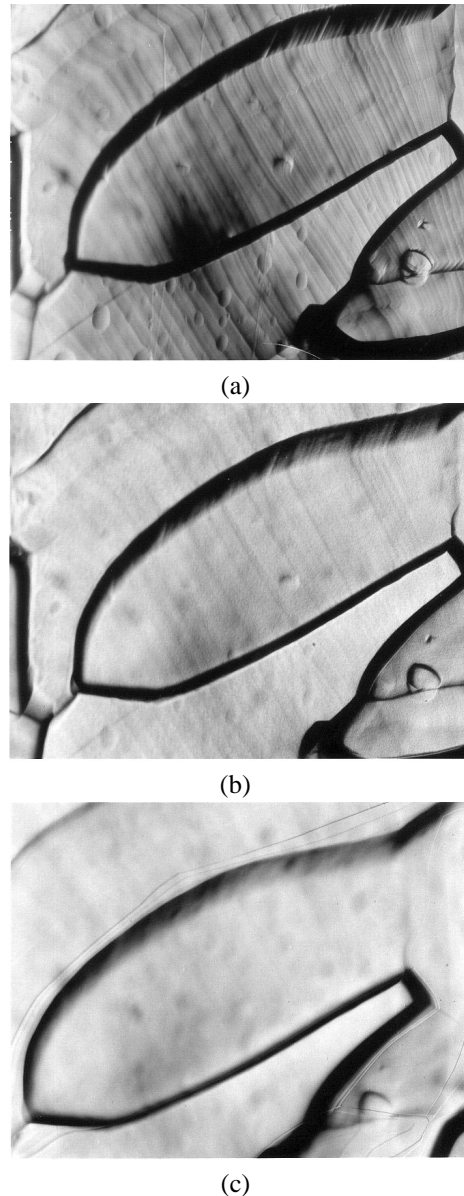
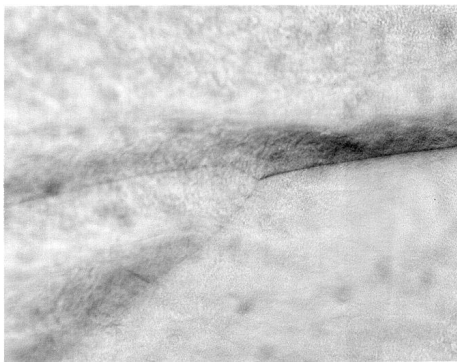


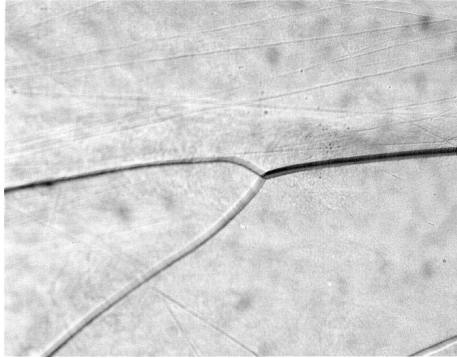
Figure 3: The weld surface of the sample TWC-155E after BCP followed by repeated EP. After a surface removal of  $117\mu\text{m}$  by BCP (a). After an extra removal of  $26\mu\text{m}$  (b);  $90\mu\text{m}$  (c) by EP. The left border of the photos coincides with the weld joint line. The tie-shaped feature dominating the photo center is a plateau with respect to the area surrounding it.

lower side in the picture. The configuration of the other two linear features is actually undercut, which is a frequently observed feature for a weld surface etched by BCP.

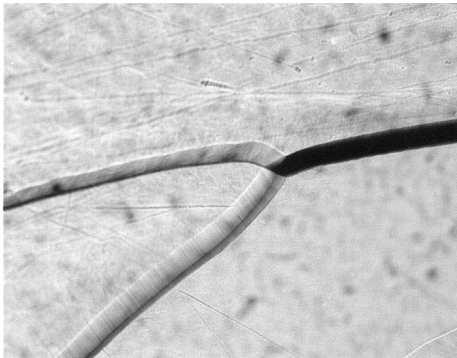
As can be seen from Fig. 4, the smooth RF surface is easily destroyed by a light BCP. An extra etching of  $12\mu\text{m}$  by BCP is sufficient to re-establish sharp edges, although the step height is not that great. Again increasing of the step height with the amount of surface removal by BCP is demonstrated.



(a)



(b)



(c)

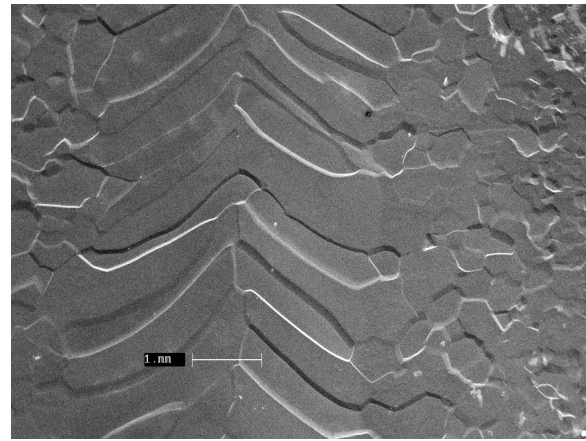
Figure 4: The weld surface of the sample S3C1-3-EQUATOR after EP followed by repeated BCP. After a surface removal of  $100\mu\text{m}$  by EP (a). After an extra removal of  $12\mu\text{m}$  (b);  $44\mu\text{m}$  (c) by BCP. The linear feature starting from the center to right is a going-down step if walking from the upper to the lower side in the picture.

## 5 EP VS BCP IN A LARGER PICTURE

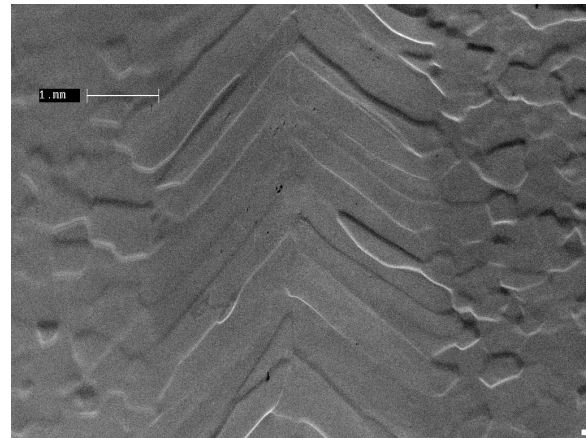
The effects of repeated BCP and EP on weld regions have been discussed in previous sections. In this section, RF surfaces of all the three regions after being well etched by BCP are comparatively presented with those being well etched by EP.

### 5.1 The weld and heat-affected region

Fig. 5(a) and (b) show low magnification SEM photos of the weld region and heat-affected region of the sample



(a)



(b)

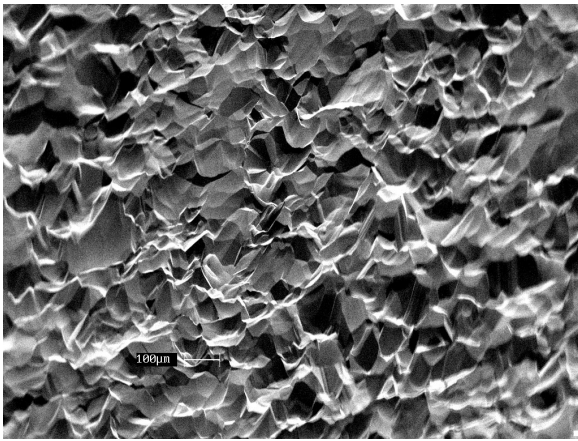
Figure 5: The RF surface of the weld and heat-affected region of the sample TWC-155E after a surface removal of  $117\mu\text{m}$  by BCP (a), and after an extra removal of  $90\mu\text{m}$  by EP. The length of scale bars in the photos is 1mm.

TWC-155E after a surface removal of  $117\mu\text{m}$  by BCP and after an extra removal of  $90\mu\text{m}$  by EP, respectively.

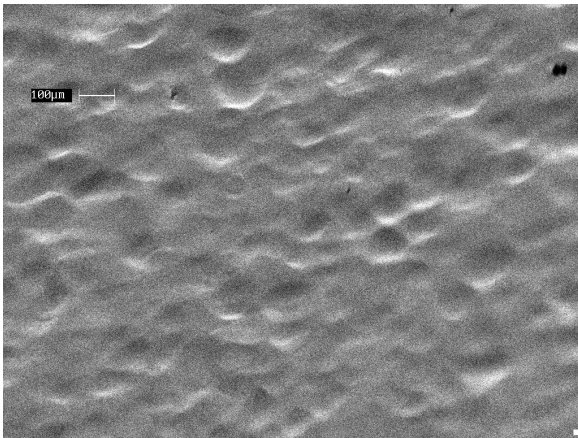
As can be seen in Fig. 5(a), there are a number of bright features, both in the weld and heat-affected region after being well etched by BCP. In contrast, after an extra etching by EP, both the number of bright features and their brightness are greatly reduced. This suggests that [5] the number of sharp edges and their sharpness are both reduced by EP. However, one should bear in mind that not all the edges are perfectly rounded off with the extra etching by EP, which means even further EP is needed to obtain an ideal weld surface.

### 5.2 The non-affected region

Fig. 6 shows the difference between the RF surface of a non-affected region after a surface removal of  $117\mu\text{m}$  by BCP and that after a further removal of  $90\mu\text{m}$  by EP. As can be seen from Fig. 6(a) the surface of the non-affected region is rather rough after the etching by BCP, whereas it is significantly smoothed out by the further EP, as shown in



(a)



(b)

Figure 6: The RF surface of the non-affected region of the sample TWC-155E after a surface removal of  $117 \mu\text{m}$  by BCP (a) and after an extra  $90 \mu\text{m}$  removal by EP. The length of scale bars in the photos is  $100 \mu\text{m}$ .

Fig. 6(b).

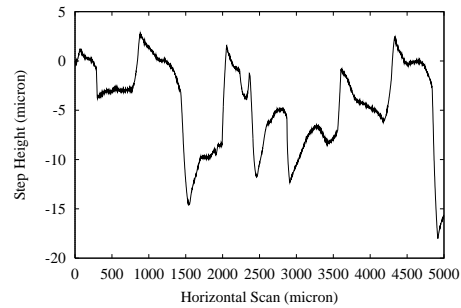
## 6 SURFACE PROFILES

As shown in previous sections, RF surfaces being well etched by BCP are characterized by steps with sharp edges in the weld and the heat-affected region and a high roughness in the non-affected region.

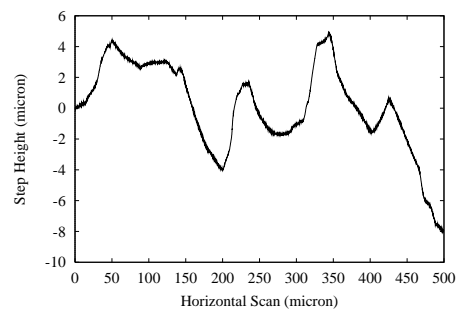
In order to have a better understanding about these surface irregularities, data in the vertical dimension are highly desired. Although the height of a particular step in the weld region can be measured with an SEM by tilting the sample, statistical data about the steps in the weld region and the roughness of the surface in a non-affected region can not be yielded effectively in this manner. Yet these data are crucial in determining the distribution function of the field enhancement factor discussed in [6]. For this reason, the surfaces of the samples were measured with a surface profiler. The stylus of the profiler used in this study (Alpha-step-500 by Tencor) has a curvature radius of  $5 \mu\text{m}$  and a shank angle of  $60^\circ$ .

### 6.1 Step height

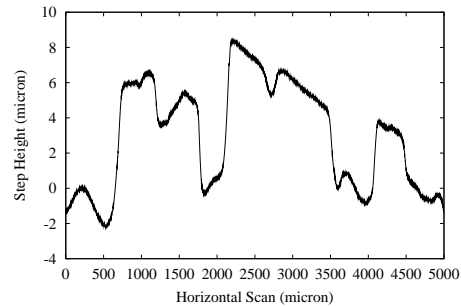
Typical surface profiles of RF surfaces in different regions being etched by different methods are shown in Fig. 7. Fig. 7(a) and (b) show profiles of the weld and non-affected



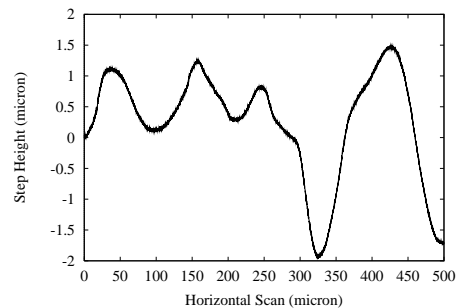
(a)



(b)



(c)



(d)

Figure 7: Surface profiles of the sample TWC-155E. The weld (a) and non-affected region (b) after a surface removal of  $117 \mu\text{m}$  by BCP. The weld (c) and non-affected region (d) after an extra  $90 \mu\text{m}$  removal by EP. Note the difference in horizontal scale for the weld and non-affected region.

region of the sample TWC-155E after a surface removal of  $117\ \mu\text{m}$  by BCP. Fig. 7(c) and (d) show profiles of the weld and non-affected region after a surface removal of  $117\ \mu\text{m}$  by BCP followed by an extra  $90\ \mu\text{m}$  surface removal by EP.

The rounding-off effect of step edges by EP is borne out again by the surface profile measurement, which is independent to the microscopic photography described in previous sections. Unfortunately, limited by the curvature radius of the stylus, curvature radius of step edges could not be resolved. An approach was developed in [6] to gauge the curvature radius of steps and an upper limit was outlined.

Despite the difficulty in curvature radius measurement, the step height can be accurately measured with the stylus used in this study. Measurements with the sample TWC-155E after repeated etching by EP reveal a gradual reduction of the step height in the weld and heat-affected region and a vigorous roughness reduction in the non-affected region. In contrast, the step height in the weld region increase significantly with repeated BCP (see the RMS step height in the following section). No step height saturation is seen up to a  $250\ \mu\text{m}$  surface removal by BCP in the weld region.

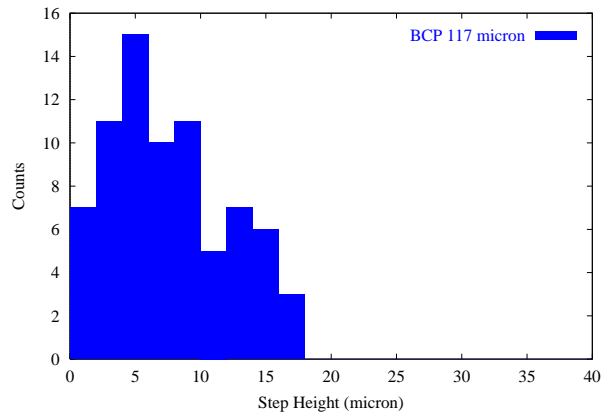
## 6.2 Step height statistics

In order to compare the surface characteristics after different surface treatments, statistical data are needed due to the fact that large number of steps with diverse configurations are involved. Here the *distribution of step height* is emphasized because of its close relationship with the distribution function of the magnetic field enhancement factor discussed in [6]. The RMS step height is cited only for a general comparison purpose.

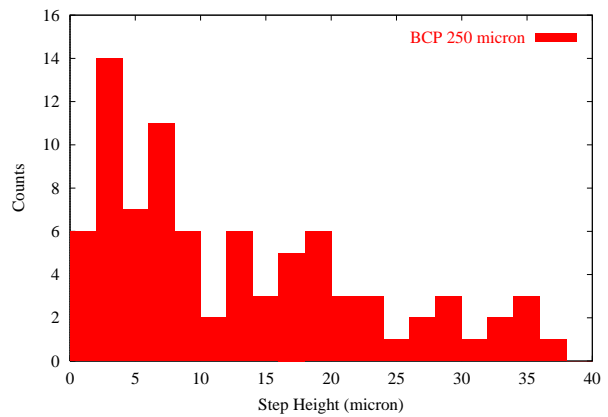
Fig. 8 depicts histograms of step height in the weld region of the sample TWC-155E after different surface treatment. Here the effects of different polishing techniques are clearly illustrated. More surface etching by BCP greatly increases the number of larger steps. The highest registered step height is even close to  $40\ \mu\text{m}$  after a surface removal of  $250\ \mu\text{m}$  ( see Fig. 8(b) ). In contrast, the number of larger steps is significantly reduced with surface etching by EP. Most steps have a height of less than  $10\ \mu\text{m}$  after an extra surface removal of  $90\ \mu\text{m}$  following an original removal of  $117\ \mu\text{m}$  by BCP ( see Fig. 8(c) ).

Fig. 9 depicts histograms of step height in the non-affected region of the sample TWC-155E after different surface treatments. Unlike in the weld region, a step height saturation is observed here in the non-affected region. The maximum and the RMS step height are nearly the same with an etching of  $117\ \mu\text{m}$  and  $250\ \mu\text{m}$  by BCP. Again, EP plays an important role in reducing the surface roughness in the non-affected region.

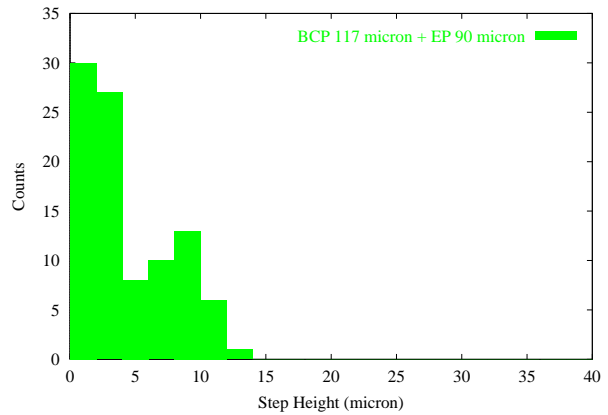
From these statistical data, one can calculate the root mean square step height, which can be used as a general gauge of the surface irregularity. Table 1 lists the root mean square step height and the maximum height in the weld region of the sample TWC-155E after different surface treat-



(a)



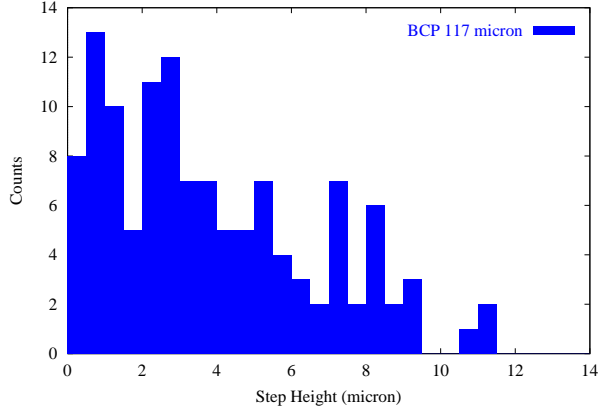
(b)



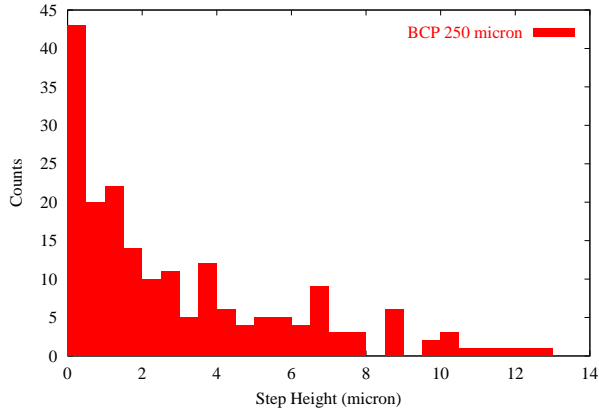
(c)

Figure 8: Histograms of step height in the weld region of the sample TWC-155E. After a surface removal of  $117\ \mu\text{m}$  (a). After a surface removal of  $117\ \mu\text{m}$  by BCP followed still by an extra  $133\ \mu\text{m}$  removal by BCP (b). After a surface removal of  $117\ \mu\text{m}$  by BCP followed by an extra  $90\ \mu\text{m}$  removal by EP (c).

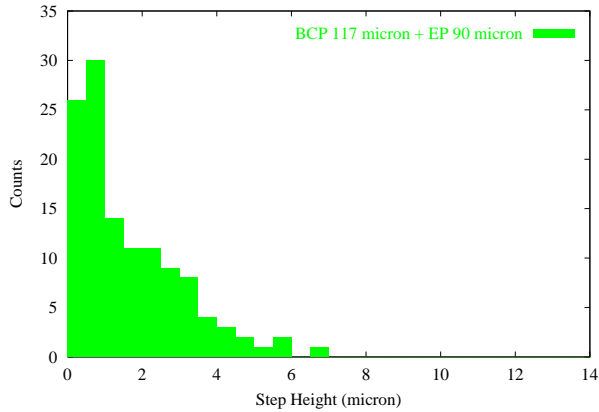
ments. Table 2 lists the root mean square step height and the maximum height in the non-affected region of the sample TWC-155E after different surface treatments.



(a)



(b)



(c)

Figure 9: Histograms of step height in the non-affected region of the sample TWC-155E. After a surface removal of  $117 \mu\text{m}$  by BCP (a);  $250 \mu\text{m}$  (b). After a surface removal of  $117 \mu\text{m}$  by BCP followed by an extra  $90 \mu\text{m}$  removal by EP (c).

## 7 DISCUSSIONS

RF surfaces of niobium experience substantial changes on the microscopic scale over the course of surface polishing. As a result, the surface may manifest some properties dif-

Table 1: Statistics of step height in the weld region of the sample TWC-155E

surface removal	RMS [ $\mu\text{m}$ ]	Max. [ $\mu\text{m}$ ]
$117 \mu\text{m}$ BCP	8.8	17.8
$250 \mu\text{m}$ BCP	16.2	36.8
$117 \mu\text{m}$ BCP + $90 \mu\text{m}$ EP	5.5	13

Table 2: Statistics of step height in the non-affected region of the sample TWC-155E

surface removal	RMS [ $\mu\text{m}$ ]	Max. [ $\mu\text{m}$ ]
$117 \mu\text{m}$ BCP	4.8	11.4
$250 \mu\text{m}$ BCP	4.3	12.6
$117 \mu\text{m}$ BCP + $90 \mu\text{m}$ EP	2.2	6.7

ferent from that of the bulk due to either morphological factors or compositional factors. Recent studies have shown that a cavity etched by BCP may suffer from high-field Q drop, whereas, after certain amount of further etching by EP, the Q drop could be removed and the quench field could also be raised [3]. Among others, a model based on the magnetic field enhancement has been developed to explain this phenomenon [6]. Studies presented in this paper have important implications in the context of the high-field Q drop of a superconducting cavity.

### 7.1 Magnetic field enhancement

Magnetic field can be enhanced locally on the surface of the corner of a step. The dependence of the enhancement factor on the curvature radius of the corner of a step has been dealt with in great detail in [6]. Preliminary simulations in a 3-D fashion with the code MAFIA [9] suggest that the field enhancement factor is also a strong function of the orientation of a step and its aspect ratio. The enhancement is maximized if the step edge is oriented to be perpendicular to the magnetic field lines, whereas the enhancement is trivial if the step edge is oriented to be parallel to the magnetic field lines. The magnetic field enhancement factor was also found to be proportional to the aspect ratio of the step. Basically, a longer or higher step will result in a stronger magnetic field enhancement factor. In this study, we found most steps in the weld region have a elongated dimension in the direction of about  $60^\circ$  away from the joint line. Magnetic field lines of the working mode in an elliptical superconducting cavity is unfortunately parallel to the joint line. As a result, steps in the weld region are more perpendicular than parallel to the magnetic field lines. For these reasons (both orientational and dimensional), a stronger magnetic field enhancement is expected in the weld region compared to in the other regions.

### 7.2 Linearity of the step

Step edges on the RF surface of a niobium can be viewed as some kind of defects in case that the local surface is driven

into normal conducting due to magnetic field enhancement. Theoretical work regarding the relationship between the breakdown field and the geometry of a defect has shown that linear defects are more vulnerable to thermal instabilities compared with circular ones [10]. As can be seen from Fig. 1, steps in the weld region of a niobium being well etched by BCP have elongated dimension in the direction of about  $60^\circ$  away from the weld joint line, and hence they are highly linear. As a result, a superconducting cavity will be more likely to quench in the EBW region than in the other regions (here we limit ourselves to a cavity working in the high gradient regime,  $> 20$  MV/m, assuming it is free from thermal breakdown and field emission). This claim goes even stronger considering the fact that the magnetic field enhancement factor is higher in the EBW region, as discussed in previous section.

### 7.3 How much etching is needed

It has been established that a surface removal of more than  $100\ \mu\text{m}$  is needed to reach an ideal accelerating gradient [7][8]. In this study, we found the RF surface in the weld region is dominated by circular defects until a surface removal of about  $120\ \mu\text{m}$  was reached. One could argue that there may be some correlation between these circular defects and cavity performance at gradients  $< 20$  MV/m.

More surface etching by BCP is helpful in eliminating these circular defects and pushing the gradient to higher levels in the  $< 20$  MV/m regime. However, aggressive surface etching by BCP beyond  $150\ \mu\text{m}$  may be unfavorable, as it will trigger the high-field Q drop when the cavity works at higher gradients ( $> 20$  MV/m). Because the step height will increase with more etching by BCP and a higher field enhancement is resulted. For this reason, we suggest an aggressive etching by BCP of more than  $150\ \mu\text{m}$  surface removal should be cautioned.

Basically surface etching by EP will round off step edges and reduce the step height on a niobium surface. Studies presented in this paper show that even after a surface removal of  $90\ \mu\text{m}$  by EP is reached, the step height is still rather high,  $\sim 10\ \mu\text{m}$ , in the weld region of a surface previously well etched by BCP. It is therefore expected that more surface removal, presumably more than  $150\ \mu\text{m}$ , is needed to smooth out a weld surface having received significant etching by BCP.

## 8 CONCLUSIONS

The RF surface in the EBW region of niobium after sufficient etching by BCP is characterized by micro-steps with sharp edges near grain boundaries. The step height increases with repeated etching by BCP and can be as high as more than  $30\ \mu\text{m}$ . No step height saturation in the weld region was seen up to a surface removal of  $250\ \mu\text{m}$ .

The steps in the weld region are lined up in a way that they form an angle of about  $60^\circ$  with respect to the weld joint line. The grains in the weld region have elongated di-

mensions in the lining-up direction, as a result their boundaries are highly linear.

The step edge is significantly rounded off and step height is appreciably reduced with extra surface etching by EP. A surface removal of more than  $150\ \mu\text{m}$  is needed to smooth out the weld region of a niobium having been previously well etched by BCP. Reversely, a smooth surface obtained by heavy EP can be easily destroyed by further BCP, even as light as a surface removal of  $12\ \mu\text{m}$ .

## 9 REFERENCES

- [1] H. Padamsee, J. Knobloch, and T. Hays, *RF superconductivity for accelerators*, Chapter 6, John Wiley & Sons, Inc., 1998.
- [2] H. Safa, *Proc. of the 8<sup>th</sup> workshop on superconductivity*, Abano Terme (Padova), Italy, 1997, p814.
- [3] E. Kako et. al., *Proc. of the 1999 Particle Accelerator Conference*, New York, USA, 1999, p432.
- [4] J. Kirchgessner, *Proc. of the 4<sup>th</sup> Workshop on RF Superconductivity*, Argonne National Lab., Argonne, IL, USA, 1998, p533.
- [5] These SEM photos were taken in the secondary electron mode with the secondary electron detector located over the top of the sample. The sample was tilted  $80^\circ$  with respect to the ground level. Photos presented in the paper have been converted with tilt correction taken into account. In this configuration, a bright feature in the photo represents a step facing towards the detector as a result of the combination of the emission contrast and detection contrast. Due to the surface sensitive nature of secondary electron emission, the brightness of a step edge can be in a way translated into its sharpness.
- [6] J. Knobloch, R.L. Geng, M. Liepe, H. Padamsee, *these proceedings*, TUA004.
- [7] P. Kneisel, *Proc. of the 8<sup>th</sup> workshop on superconductivity*, Abano Terme (Padova), Italy, 1997, p830.
- [8] K. Saito et. al., *Proc. of the 8<sup>th</sup> workshop on superconductivity*, Abano Terme (Padova), Italy, 1997, p795.
- [9] A step-loaded rectangular cavity, big enough compared with the dimension of the step, was used to simulate the magnetic field enhancement effect with different step orientations.
- [10] N. A. Buznikov and A. A. Pukhov, *Supercond. Sci. Technol.*, 11(1998), P1201-1208.